Supplementary Information

High tunneling magnetoresistance induced by symmetry and quantum interference in magnetic molecular junctions

Lin Huang[1], Yu-Jia Zeng[1], Dan Wu[2], Nan-Nan Luo[1], Ye-Xin Feng[1], Zhi-Qiang Fan[2], Li-Ming Tang[1], Ke-Qiu Chen[1*]

[1]*Department of Applied Physics, School of Physics and Electronics, Hunan University, Changsha 410082, China*

[2]*Hunan Provincial Key Laboratory of Flexible Electronic Materials Genome Engineering, School of Physics and Electronic Science, Changsha University of Science and Technology, Changsha 410114, China.*

1. Effects of coupling strength between the molecule and electrode on transport

The spin-resolved transmission spectra of the MTJs with different interfacial distance are shown in Fig. S4. Here, the interfacial distance d is defined as the distance from the S atom to the Ni electrodes surface. Taking the parallel spin configurations of symmetric and asymmetric MTJs as an example, we can see that the molecular orbitals are shifted to higher energies with the interfacial distance increasing. Besides, the transmission peaks above the E_F of the minority spin channel become narrower as the interface distance increases. Meanwhile, the transmission coefficients near the E_F get diminished due to the weaken hybridization between the molecule and electrode as the distance. For the asymmetric MTJs, we can also notice that the electron transmission at the dip of DQI feature in majority spin channel gets more severe suppressed as the distance increases. As the distance continues to

increase, the hybridization between the molecule and the electrode will be further weakened.

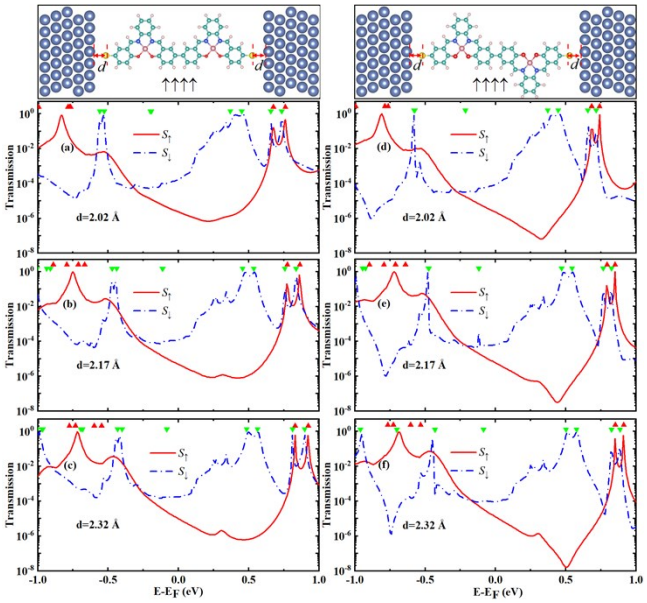

Fig. S1 (Color online). Spin resolved transmission spectra for (a)-(c) symmetric and (d)-(f) asymmetric MTJs with different interfacial distance under parallel spin configuration. Eigenvalues of molecular orbital for majority and minority spin channels are denoted as red and green triangles.

2. Spin-resolved transmission spectra of symmetric and asymmetric molecular junctions

The spin-resolved transmission spectra of symmetric/asymmetric molecular junctions under spin configuration of ↑↑↓↑ and ↑↑↑↓ are presented in Fig. S1. It can be noticed that the transmission spectra for symmetric and asymmetric conformations show similar with the parallel spin configurations (↑↑↑↑) in the main text Figs. 1(c)-(d). It means that the quantum interference can be existed under the ferromagnetic state of molecule junctions and show independent with the magnetic order of electrodes.

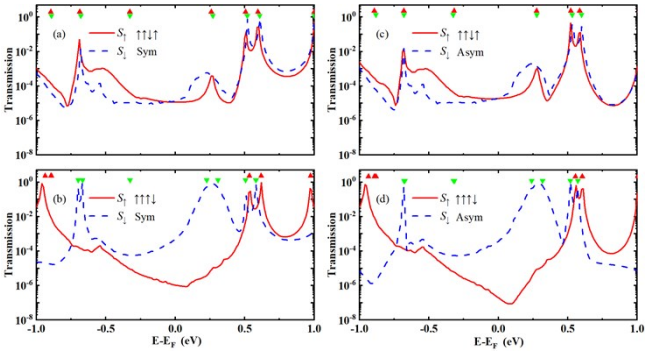

Fig. S2 (Color online). Spin resolved transmission spectra for (a)-(b) symmetric molecular junction and (c)-(d) asymmetric molecular junction under spin configuration of ↑↑↓↑ and ↑↑↑↓. Eigenvalues of molecular orbital for majority and minority spin channels are denoted as red and green triangles.

3. Spin-resolved transmission spectra for the MTJs formed by Fe and Co electrodes

The calculated spin-resolved transmission spectra of MTJs formed by Fe and Co electrodes are shown in Figure S2 and Figure S3. It can be seen that the quantum interference features (CQI/DQI) can still exist in the majority spin channel of parallel spin configurations. This means the quantum interference phenomenon is the intrinsic properties of the conjugated molecules and shows independence with the types of ferromagnetic electrodes. Besides, we can also note that the HOMO-LUMO gap in the Fe and Co electrodes systems is smaller than the Ni electrode system due to the stronger bonding between the molecule and electrode.[1]As a result, we can anticipate a larger conductance in Fe and Co electrodes system. For the MTJs system formed by Fe electrodes, the transmission spectrum of minority spin channel gets oscillation in the HOMO-LUMO gap (see Figures S2). While the transmission spectrum of Co electrode system shows similar with the Ni electrode system (see Figures S3). Among the three types of electrodes, the more unfilled *d* electrons in Fe atoms ($3d_6 4s^2$) will be hybridized with the molecular orbitals via the strong bonding between molecule and electrode resulting in the obvious shift of molecular orbitals.

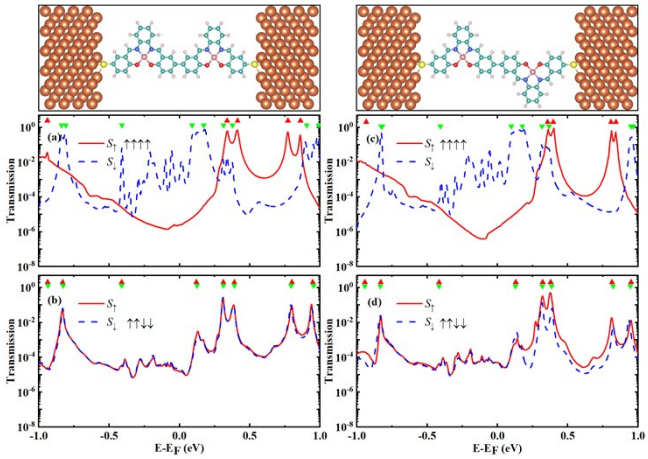

Fig. S3 (Color online). Spin resolved transmission spectra for (a)-(b) symmetric and (c)-(d) asymmetric MTJs formed by Fe electrodes (bcc, 111) under parallel and antiparallel spin configurations. Eigenvalues of molecular orbital for majority and minority spin channels are denoted as red and green triangles.

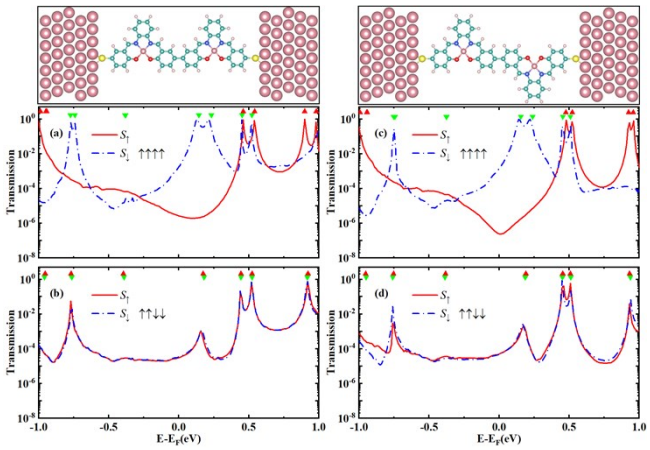

Fig. S4 (Color online). Spin resolved transmission spectra for (a)-(b) symmetric and (c)-(d) asymmetric MTJs formed by Co electrodes (fcc, 111) under parallel and antiparallel spin configurations. Eigenvalues of molecular orbital for majority and minority spin channels are denoted as red and green triangles.

4. Effects of interfacial hybridization between molecule and electrode on transport

We calculated the spin-resolved PDOS of MTJs before and after the CoSal molecule bridging and the respective difference of PDOS in electrode as shown in Fig. S5. For the isolated CoSal molecule, the molecular energy levels are discrete as

given in the Figs. S5(c)-S5(d). Owing to the scale of the MTJs up to 3nm, the interaction between the electrodes can be ignored. For the MTJ without molecular bridging, the current spin-polarization is dominated by the electrode DOS of minority spin channel ($S_{\downarrow}$). When the molecule is brought into contact with the ferromagnetic electrode, the interfacial interaction between the molecule and ferromagnetic electrode come into being. The PDOS of the bridged molecule will be modified in two ways. [2]First, the molecular orbitals near the E_F will be broadened and hybridized with *d*-orbitals of the electrodes (see Figs. S5(e)-S5(d)). Second, the molecular orbitals will be shifted due to the strong π-*d* hybridization and charge transfer between molecule and electrode. By comparing with the isolated molecule orbitals, we found an energy shift (~50meV) occurred in the minority spin channel after contacted with the electrodes. It can be a very minor energy shift which can even be ignored for the broaden of molecular orbitals exist. However, we can observe obvious energy shift in the MTJs whose electrodes formed by Fe and Co (see the Figs. S2-S3). Besides, the impart of molecule-induced coupling on ferromagnetic electrodes can be clearly seen in the Figs. S5(g)-S5(h). For the PC, there is no doubt that the hybridization between the molecule and electrode enhances the PDOS of minority spin channel in electrodes. Moreover, we can also observe the other PDOS peaks of hybridization like the sharp PDOS at -0.5 eV in the majority spin channel (caused by ferromagnetic-S hybridization) and the PDOS far away the E_F in the same majority spin channel, but these peaks which away E_F cannot contribute to the transport.

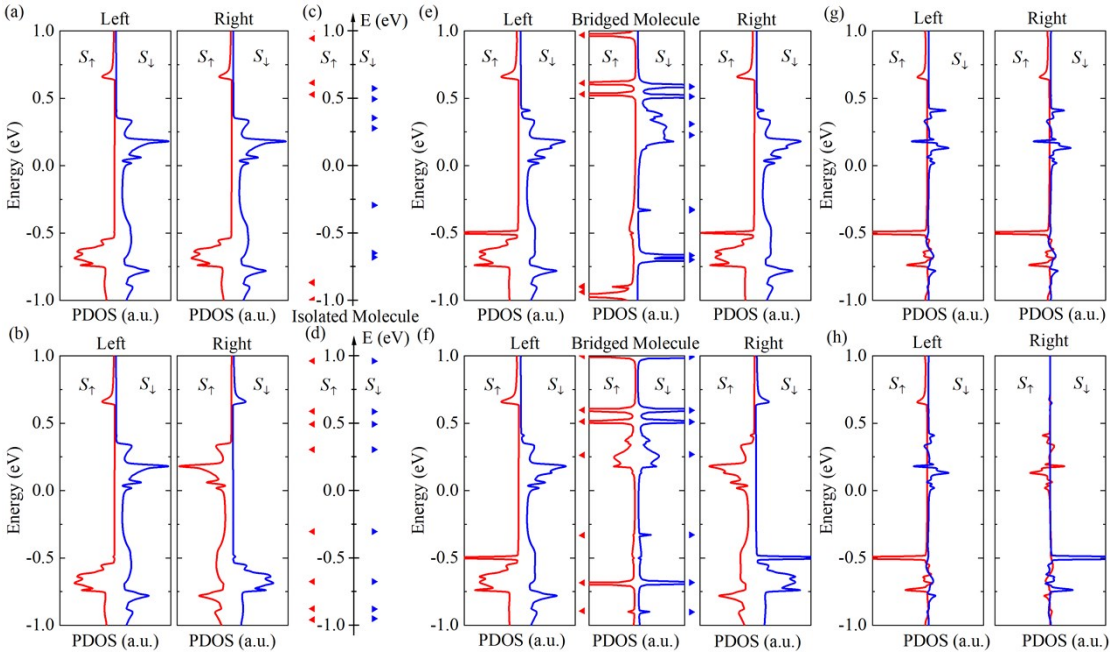

Fig. S5 (Color online). Spin-resolved PDOS of MTJ (a)-(b) before and (e)-(f) after bridging the molecule under PC/APC, (c)-(d) show the molecular energy levels of isolated symmetric CoSal molecule, (g) and (h) represent the difference between the PDOS of the respective electrodes before and after bridging the molecule. The upper panel represents the results of ferromagnetic and PC, the bottom panel shows the inverse case. Eigenvalues of molecular orbital for majority and minority spin channels are denoted as red and blue triangles.

5. Orbital symmetry analysis

Based on the Green's functions method, an electron incident on a molecular junction via molecular orbitals (MOs) can be calculated by the transmission formula $T(E) = \mathrm{Tr}(\mathbf{\Gamma}_L \mathbf{G} \mathbf{\Gamma}_R \mathbf{G}^{\dagger})$. By transforming the atomic orbital basis into the MO basis, the transmission expression can be further written as

$$T(E) = \sum_i T_i + \sum_{i<j} T_{ij} \qquad \text{(S1)}$$

Here the first term represents the noninterfering term for independent MO, which can be described by Lorentzian transmission function

$$T_i(E) = \frac{\gamma_{iL}\gamma_{iR}}{(E-\varepsilon_i)^2 + \gamma_i^2} \qquad \text{(S2)}$$

where the E is the energy of the incident electron, ε_i is the energies of Lorentzian peak for the ith MO, and $\gamma_{i\{L/R\}}$ denotes the strength of the coupling between the ith orbital and the left/right electrodes, and $\gamma_i = (\gamma_{iL} + \gamma_{iR})/2$. The second term T_{ij} represents the interfering term which can be expressed as

$$T_{ij} = 2\sqrt{T_i T_j}\cos(\psi_{ij} - \Theta(E)) \qquad \text{(S3)}$$

$$\psi_{ij} = \arg(v_{iL} v_{iR}^* v_{jL}^* v_{jR}) \qquad \text{(S4)}$$

$$\Theta(E) = \arg((E - z_i)(E - z_j^*)) \qquad \text{(S5)}$$

where the ψ_{ij} and Θ are the two angles which controlling the interference effects. $v_{L/R}$ is the effective hybridization matrix elements between the molecule and left/right electrodes. $z_{i/j}$ denote to the orbital position of ith and jth.

In the weak coupling limit, the broadening strength is far below the separated resonance positions ($\gamma_{ij} = |\varepsilon_j - \varepsilon_i|$). The term of $\cos(\psi_{ij} - \Theta)$ can be written as

$$\cos(\psi_{ij} - \Theta(E)) = \text{sign}(\mathrm{v}_{iL}\mathrm{v}_{iR}\mathrm{v}_{jL}\mathrm{v}_{jR})\cos\Theta(E) \qquad \text{(S6)}$$

Since in the valley region of transmission spectrum, the Θ is close to π. Thus, we have $\psi_{ij} \approx 0$ when the destructive quantum interference (DQI) occurs, while at $\psi_{ij} \approx \pi$ it corresponds to the constructive quantum interference (CQI).

As discussed in the main text (see Figure 3), the orbitals of isolated molecular junctions for symmetric and asymmetric conformations are demonstrated have the features of CQI and DQI, respectively. The positions of highest occupied molecular orbital (HOMO), HOMO-1, HOMO-2 for isolated molecular junctions are close to each other. The HOMO-1 and HOMO-2 of majority spin are degenerate $3d_z^2$ orbitals. When the molecules are coupled to the electrodes, due to the strong interaction in the interface of molecule/electrode and the charge transfer from the Ni electrodes to molecule, the two-degenerate d orbitals with $3d_z^2$ are shifted to the position of HOMO. As shown in Figures S6-S7, the HOMO and HOMO-1 of majority spin are

strongly localized in the Co atoms with $3d_z^2$ spatial symmetry which have no contribution to the electron transport due to the σ-type orbital (see the transmission spectrum in Figures 1(c)-1(d)). Besides, we can also note the π-type for the rest orbitals especially for the two orbitals lowest unoccupied molecular orbital (LUMO) and LUMO+1 which constitute the main conduction channel for both molecular junctions. For both spin channels of symmetric MJ, the relative phase shift between the orbitals of HOMO-2 and LUMO is $\psi_{ij} \approx \pi$ which correspond to the constructive quantum interference discussed in the main text. In addition, for the asymmetric molecular junction, the relative phase shift between the HOMO-2 and LUMO of the majority channel is $\psi_{ij} \approx 0$, which agree with the destructive quantum interference result in the main text. For the minority spin channel, the relative phase shift between the two orbitals is $\psi_{ij} \approx \pi$. Thus, the orbital symmetry analysis shown in the main text is feasible.

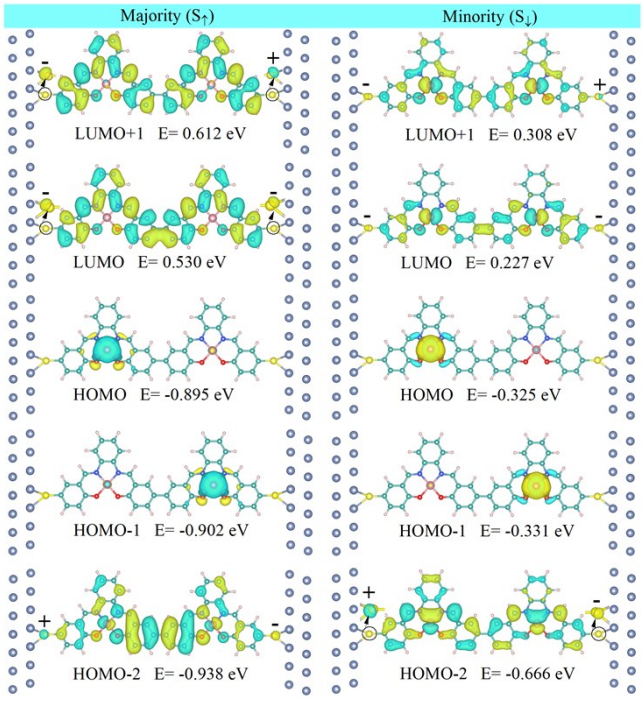

Fig. S6 (Color online). Spatial distributions of spin-dependent frontier MPSH molecular orbitals of Co-Salophene molecular junctions with symmetric conformations in parallel spin configuration (isovalue=0.012). Majority and minority

spin channel are showed in the left and right panel respectively. Green regions: positive sign, yellow regions: negative sign. To get a clear picture, a small isovalue 0.005 is set to give the details on S atoms.

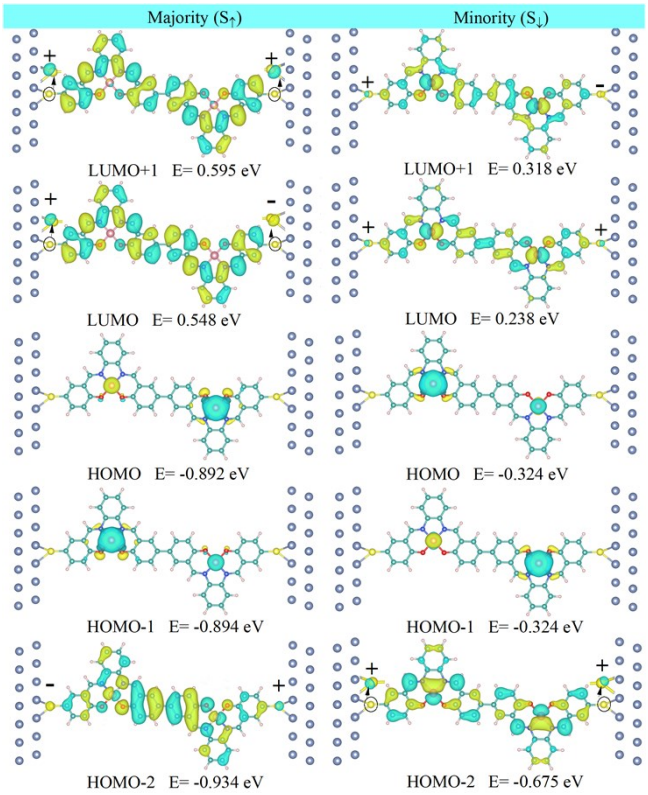

Fig. S7 (Color online). Spatial distributions of spin-dependent frontier MPSH molecular orbitals of Co-Salophene molecular junctions with asymmetric conformations in parallel spin configuration (isovalue=0.012). Majority and minority spin channel are showed in the left and right panel respectively. Green regions: positive sign, yellow regions: negative sign. To get a clear picture, a small isovalue 0.005 is set to give the details on S atoms.

6. Spin-resolved transmission pathway of PC (↑↑↑↑) for symmetric and asymmetric conformations

As shown in Figure S8, the spin-resolved transmission pathways of symmetric and asymmetric molecular junctions were calculated at the energy positions of 0.15eV and 0.06eV, respectively. It can be seen that the transmissions of electrons are strong

scattered at Co atoms in the majority spin channel. For the asymmetric molecular junction, it can be clearly seen that the transmission pathways exhibit backscattering process which means destructive quantum interference (see the transmission pathway at the interface of molecule and electrodes). While for the minority spin channel, the electrons are mainly transmitted through the backbone of the CoSal molecule, showing large forward transmission.

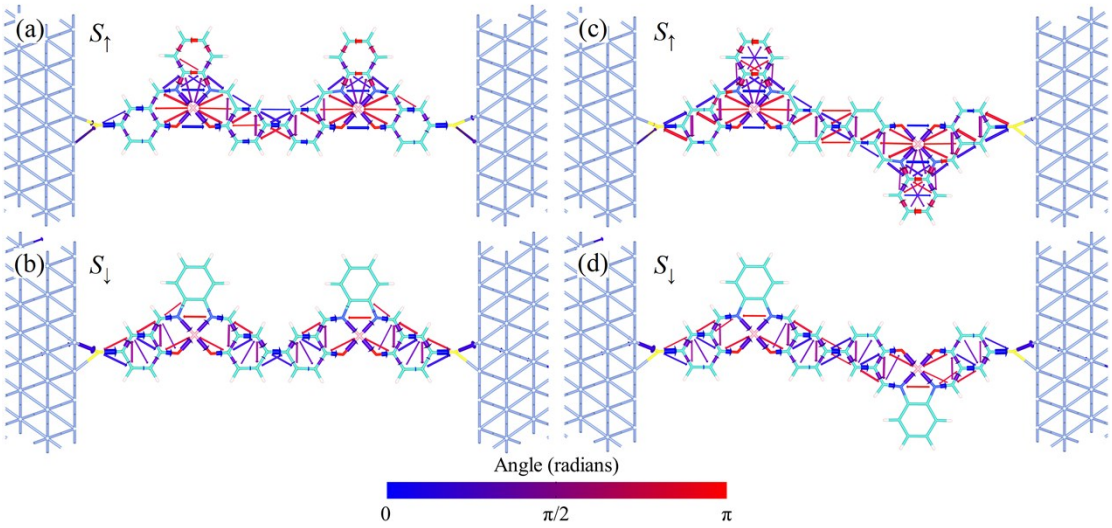

Fig. S8. (Color online) Spin resolved transmission pathways for (a)-(b) symmetric molecular junction and (c)-(d) asymmetric molecular junction under parallel spin configuration.

References

1. A. Aadhityan, C. P. Kala and D. J. Thiruvadigal, *Appl. Surf. Sci*, 2017, **418**, 393-400.

2. S. Sanvito, *Nat. Phys.*, 2010, **6**, 562-564.